FEBS Letters 477 (2000) 278–282 FEBS 23930

ATPase cycle controls the conformation of an archaeal chaperonin as visualized by cryo-electron microscopy

Irina Gutsche*, Oana Mihalache, Reiner Hegerl, Dieter Typke, Wolfgang Baumeister

Max-Planck-Institute for Biochemistry, Am Klopferspitz 18a, D-82152 Martinsried, Germany

Received 17 April 2000; revised 31 May 2000; accepted 31 May 2000

Edited by Matti Saraste

Abstract Chaperonins are double-ring protein folding machines fueled by ATP binding and hydrolysis. Conformational rearrangements upon ATPase cycling of the group I chaperonins, typified by the *Escherichia coli* GroEL/GroES system, have been thoroughly investigated by cryo-electron microscopy and X-ray crystallography. For archaeal group II chaperonins, however, these methods have so far failed to provide a correlation between the structural and the functional states. Here, we show that the conformation of the native αβ-thermosome of *Thermoplasma acidophilum* in vitrified ice is strictly regulated by adenine nucleotides.

Key words: Chaperonin; Thermosome; Cryo-electron microscopy; ATPase cycle; *Thermoplasma acidophilum*

1. Introduction

Chaperonins are ubiquitous double-ring assemblies with a central cavity that provides a compartment for ATP-driven folding of proteins [1,2]. Non-native substrates are captured by the open hydrophobic cavity of the apo-chaperonin to prevent aggregation and to partly unfold kinetically trapped intermediates. ATPase cycling triggers a series of conformational rearrangements of the chaperonin: the cavity closes, turning into a hydrophilic Anfinsen cage that gives the encapsulated substrate an opportunity to fold, and re-opens to allow substrate release.

The exact relationship between the nucleotide-bound state and the conformation of the folding machine has so far only been understood for the group I chaperonins from bacteria and endosymbiotic organelles, typified by the *Escherichia coli* heat-shock protein GroEL. In contrast, it remains elusive for the group II members from archaea and the eukaryotic cytosol-thermosome and t-complex polypeptide 1 ring complex (TRiC)/chaperonin containing t-complex polypeptide 1 (CCT) respectively [3]. In GroEL, the transition between the two major states is induced by an interplay of ATP with a single-ring co-chaperonin GroES. Their binding to the same ring as the non-native protein results in a displacement of the latter into the cavity and the closure of the folding compartment by the GroES lid. Subsequent hydrolysis of ATP enables ATP binding to the opposite ring, which triggers GroES and substrate release. However, instead of a detachable GroES-like cofactor, the group II chaperonins possess a built-in lid provided by protrusions of the apical domains of the chaperonin itself [4,5]. Furthermore, the difference in the inter-ring contacts in GroEL [6,7] and in thermosome [5] or TRiC [8] suggests that the allosteric regulation of the ring communication by adenine nucleotides, established for the group I chaperonins, is not applicable to their group II relatives.

In the case of TRiC/CCT, cryo-electron microscopy (cryo-EM) data seem to indicate a behavior similar to the GroE system. Indeed, TRiC/CCT has a typical cylindrical shape in the absence of nucleotides but becomes asymmetric, with one ring open and the other closed, upon incubation with ATP [8]. However, characterization of the structural states of the thermosome during the functional cycle has been hampered by difficulties in inducing conformational changes by nucleotide binding both in 3-D crystals and in vitrified ice. On the one hand, the apo-thermosome from *Thermoplasma acidophilum* appears in an open double-doughnut conformation in cryo-EM [9] and in a closed, nearly spherical conformation in X-ray crystallography [5]. Our recent analysis of the thermosome rearrangements in solution by small-angle neutron scattering (SANS) provided clear evidence that the crystallization buffer, containing 2 M $(NH_4)_2SO_4$, was sufficient to induce the closure of the chaperonin [10]. Together with the constraints of the crystal packing, this might be a reason why soaking of different nucleotides into the crystal leaves the lid domain unaltered. On the other hand, already in the absence of nucleotides, the apo-thermosome from another archaeon, *Sulfolobus shibatae*, in vitrified ice was recently found to occur as a mixture of three different conformations: open (45%), closed (25%), and asymmetric (30%). Even more surprisingly, no shift in the distribution of these conformations could be achieved by incubation of the protein with adenine nucleotides at 60°C [11]. The authors explain this inability to switch between the different conformations by the necessity of vitrifying the preparation from room temperature. Inconsistent with this view, SANS analysis demonstrates that *T. acidophilum* thermosomes do respond to alternations in the nucleotide-bound state by conformational rearrangements at 10 or 20°C, as well as at the physiological temperature of 55°C. Originally, in order to interpret the resemblance of the crystal structure of the *T. acidophilum* thermosome to the GroEL-GroES-ATP complex, the closure of the protrusions of the group II chaperonins was suggested to be triggered by binding of ATP [5,12]. Unexpectedly, only a slight enlargement of the open apo-chaperonin upon ATP binding was revealed by SANS, whereas a closure could be observed in the presence of ADP and Pi, which we proposed to mimic the thermosome-

*Corresponding author. Fax: (49)-89-8578 2641.
E-mail: gutsche@biochem.mpg.de

Abbreviations: CCT, chaperonin containing t-complex polypeptide 1; TRiC, t-complex polypeptide 1 ring complex

PII: S0014-5793(00)01811-1

ADP-Pi hydrolytic intermediate [10]. In this work, we provide evidence that in vitrified ice, as well as in solution, ATPase cycle exerts a strict control over the conformation of the *T. acidophilum* thermosome.

2. Materials and methods

2.1. Materials

All reagents were analytical grade. ATP, ADP, complete protease inhibitor cocktail tablets were from Boehringer Mannheim, DNase I was from Sigma.

2.2. Protein preparation

For the isolation of native thermosomes from *T. acidophilum*, cells were grown as described [13] and the chaperonin was purified using modifications of published procedures [5,13]. The purification took place at 4°C. About 30 g cells (wet mass) were resuspended in two volumes of buffer A (20 mM Tris–HCl, pH 7.5, 150 mM NaCl, 1 mM EDTA, 2 mM NaN_3 and 5% glycerol) supplemented with 5 mM $MgCl_2$, 1 antiprotease tablet and 0.1 mg/ml DNase I. Lysis was initiated by adjustment of pH to 7.5 with 3 M Tris–HCl, pH 9.5. Complete disruption was achieved with a homogenization in a douncer followed by a brief sonication. After centrifugation for 30 min at $50\,000\times g$ and 30 min at $85\,000\times g$, the supernatant became transparent and could directly be loaded onto a 4 l Sephadex 6B gel filtration column equilibrated in buffer A. High molecular weight fractions were analyzed by SDS–PAGE [14]. Pooled fractions containing thermosome were applied to a Fractogel EMD DMAE-600S column (20 ml, resin from Merck) equilibrated in buffer A without EDTA (buffer B). The column was washed with buffer B, and proteins were eluted with a 200 ml linear gradient of 0–250 mM NaCl in the same buffer. Thermosome containing fractions were loaded onto a 20 ml hydroxyapatite column (Macroprep ceramic hydroxyapatite 40 μm, Bio-Rad) equilibrated in buffer C (50 mM KH_2PO_4/K_2HPO_4, pH 7.5, 5% glycerol). Fractions, pooled after elution with a 200 ml linear gradient of buffer C with 50–400 mM phosphate, contained pure thermosome. To eliminate eventual aggregates and/or dissociated material, it was next applied to a 350 ml Superose 6 gel filtration column equilibrated in buffer D (20 mM Tris–HCl, pH 7.5, 150 mM NaCl, 10 mM $MgCl_2$, 1 mM EDTA, 1 mM DTT, 2 mM NaN_3 and 5% glycerol). Finally, the peak corresponding to double-toroidal thermosomes was concentrated by ultrafiltration up to 10–50 mg/ml (Pall Filtron Jumbosep and Macrosep, cutoff 30 kDa). Typically, the yield was around 1 mg protein per gram cells. HPLC analysis revealed that αβ-thermosomes obtained according to these procedures were in their apo-form, i.e. ATP/ADP-free. The pure chaperonin was analyzed by negative stain EM to confirm the structural integrity of the particle and tested for its capacity for ATP binding and hydrolysis.

2.3. Cryo-EM and image processing

Prior to electron microscopy, concentrated protein was diluted to 0.1 mg/ml in 20 mM Tris–HCl, pH 7.5, 15 mM $MgCl_2$. Holey carbon film was rendered hydrophilic in a Plasma cleaner (Harrick Scientific Corporation, NY, USA). A 2.5 μl droplet of protein solution was applied to the grid for about 30 s, blotted with filter-paper and rapidly plunged into liquid ethane as described by Dubochet et al. [15]. The vitrified specimens were transferred under liquid nitrogen to a Gatan cryo-holder and observed with a Philips CM 200 FEG transmission electron microscope at 160 kV. Low electron dose images were recorded on Agfa films at $34\,800\times$ magnification and digitized on a Flextight Precision 2 scanner (Imacon, Denmark) with 15.9 μm spacing, corresponding to 0.46 nm pixel size at the specimen level. The defocus of the images used for further analysis was approximately 2.5 μm as determined from the power spectra. Image processing was carried out on SGI workstations using the EM software package [16]. The images were CTF-corrected by phase-flipping of the Fourier coefficients in the negative transfer regions. From these images, subframes of 64×64 pixels containing single particles (3642 particles for apo-thermosome, 5288 for ATP-thermosome, 2392 for ADP-thermosome, 3322 for the stationary state of hydrolysis, see Section 3) were extracted interactively. A stack of images was created and the particles were translationally and rotationally aligned in an iterative way using the normalized projection of the original stack as a first reference. The aligned data sets were subjected to multivariate statistical analysis. Images were classified according to the set of significant eigenimages and subsequent averaging was performed for each class separately. Examination of the averages revealed that particles were classified mainly according to their tilt angle with respect to the imaging direction. In order to thoroughly extract the upright particles, the most symmetric (i.e. the most 'top view-like') class-average and several tilted class-averages were used for multireference alignment of the most 'top view-like' class followed by a new classification. This procedure was reiterated until no further tilted particles could be extracted from the final class of top-views. The average of this class was considered to represent the true top-view projection. Model calculations of different projections of the tomographic reconstruction of the open form of the a-only thermosome [9] revealed that similar particles which would deviate from the upright orientation by more than approximately 3° could be unambiguously separated by this procedure and at the resolution of the present work.

3. Results and discussion

The aim of this work was to discriminate between different nucleotide-bound states the thermosome undergoes during its ATPase cycling. MgATP- and MgADP-thermosome species were obtained by a 2 min incubation of the chaperonin with 15 mM ATP or ADP at 4°C, temperature at which binding takes place without being followed by measurable hydrolysis [17]. In addition, as neutron scattering measurements point to a transient closure of the chaperonin after ATP cleavage but before release of the γ-phosphate [10], we attempted to trap the chaperonin at the steady-state of hydrolysis by vitrification after incubation with 15 mM ATP for 15 min at the physiological temperature of 55°C. Since the samples could only be vitrified from room temperature, the droplets of all samples had the same temperature immediately prior to vitrification.

Regardless of the preparation, no particle images in our cryo-EM micrographs could be unambiguously assigned to side-views or highly tilted views. This may be due to the hydrophobic character of the apical domain protrusions [4], which might be attracted by the water–air interface. Accordingly, no 3-D reconstruction via angular reconstitution was attempted at this stage. Instead, we focused on establishing a correlation between the top-view appearance and the exact nucleotide-bound state. To this end, the upright particles were selected by iterative multireference alignment in conjunction with eigenvector–eigenvalue analysis, as described in Section 2. Remarkably, in the four preparations, the resulting averaged top-views of the chaperonin manifest significant differences which can be readily visualized in Fig. 1. In order to facilitate a direct comparison of the processed data with the original images (Fig. 1a–d), the protein is systematically represented in dark gray.

The top-view average of the apo-thermosome depicts a ring of orange section-shaped subunits surrounding a large cavity (Fig. 1e,i); the four-fold symmetry of the particle, discernible by eye, is confirmed by the eigenvector analysis. This image corresponds to the previously described projection of the apo-thermosome of *T. acidophilum* [18]. Without a notable change in dimensions, ATP binding drives a rearrangement of this top-view into a flower-like octagonal structure (Fig. 1f,j). A comparison between the former structures and the ADP-bound species reveals a progression from a quasi eight-fold to a clearly four-fold symmetric particle (Fig. 1h,l). Furthermore, although similar to the projection of the ATP-thermosome, ADP-chaperonin appears to have a slightly smaller in-

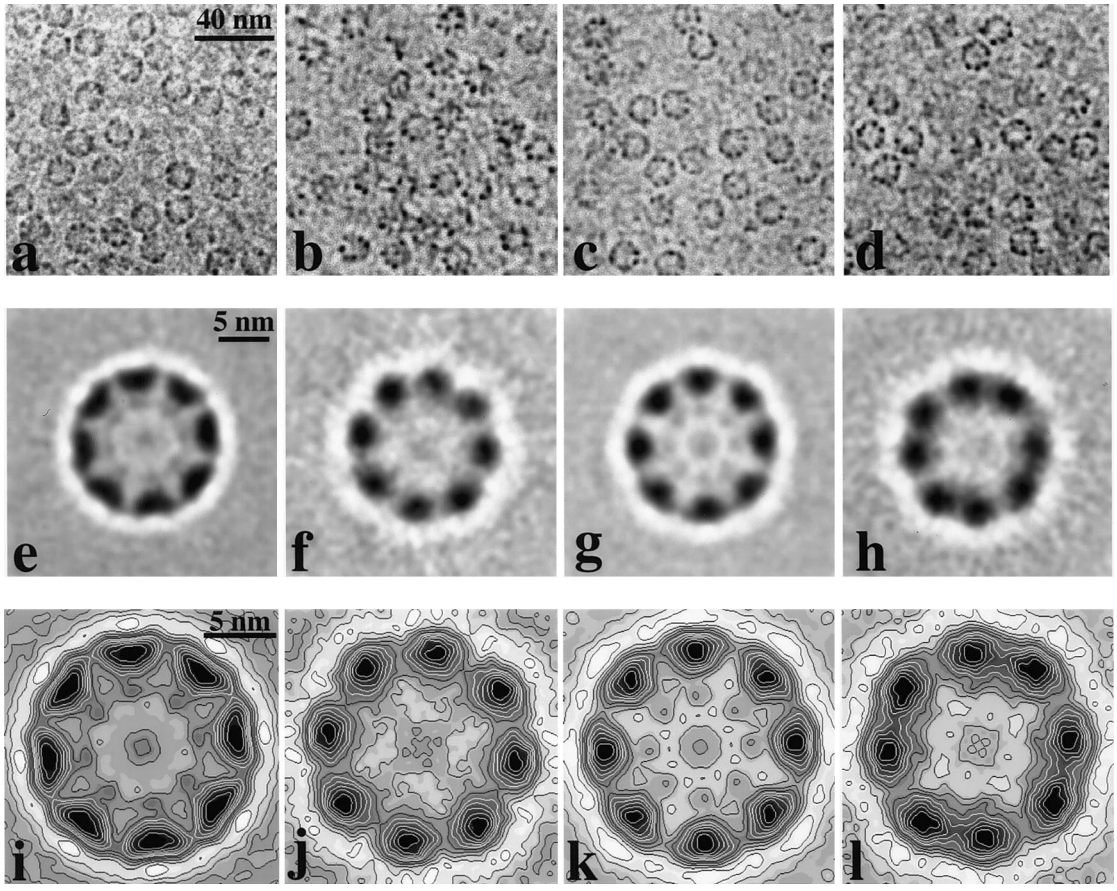

Fig. 1. Distinct conformations of different nucleotide-bound states of the thermosome. a–d: Transmission cryo-electron micrographs of (a) apo-thermosome, (b) ATP-bound state, (c) stationary state of ATP hydrolysis, (d) ADP-bound state. Iterative multireference alignment and multivariate statistical analysis allow an accurate extraction of the upright particles subjected to further analysis. e–h: Non-symmetrized 2-D averages of the extracted top-views of (e) 1257 apo-thermosome particles, (f) 310 ATP-thermosome particles, (g) 623 transient hydrolytic species, (h) 472 ADP-thermosome particles. i–l: four-fold symmetrized 2-D averages of the top-views in e–h respectively, presented as contour plots.

ner diameter and gives a more compact impression. The accentuation of the four-fold symmetry of the top-view upon nucleotide binding is in line with the previously described differences in nucleotide interaction with the α and β-subunits of the heterooligomeric chaperonin [17]. At the steady-state of hydrolysis, one would expect the protein to be present as a mixture of different nucleotide-bound states. In agreement with the observation that the rate-limiting step of the cycle is an isomerization before release of phosphate [10], most of the particles were found to be trapped in an 'ATP-like' conformation. However, armed with the knowledge about the appearance of the apo-, ATP-, and ADP-forms, we could easily identify a novel class of top-views, representing a presumed transient hydrolytic species (Fig. 1g,k). The triangular shape of its projected subunits facilitates a distinction of this tyre-like projection from those of the other states.

Thus, already the analysis of top-views allows a discrimination between different nucleotide-bound states of the thermosome, each having a distinct conformation. Yet, side-views would be necessary to envisage the structure of these states in three dimensions. The side-view projections of the native αβ-thermosome were previously found to be similar to those of the recombinant α-only thermosome, described as an open structure by cryo-electron tomography [9]. But what about the ATP-, ADP-, and the transient state, are they open, closed, or asymmetric? At least for the ATP-thermosome, the answer to this question is provided by a careful inspection of the class-averages after the first alignment and classification steps. Indeed, the unprocessed image of the ATP-bound particles seems, at first glance, very different from the others (Fig. 1b). However, we suspected that in this case the true structural differences might have been partly obscured by a pronounced deviation from the top-view orientation. Therefore, we compared the experimentally obtained class-averages with calculated projections of the closed crystal structure of the αβ-thermosome [5], the open cryo-EM structure of the α-only thermosome [9] and a hybrid structure with one ring open and the other closed. Remarkably, this analysis not only supported our hypothesis, but also revealed that only an open structure of the ATP-thermosome would account for the observed tilted projections (Fig. 2). According to these model calculations, up to 20° tilting was detected in the ATP-thermosome data sets.

Noteworthy, SANS data also indicated an open ATP-thermosome structure and even suggested a slight expansion of the particle as compared with the apo-thermosome; the radius of gyration changed from 71.9 ± 0.5 Å to 73.5 ± 0.6 Å upon ATP binding [10]. This observation, which contradicted the GroE-based assignment of the crystal conformation of the thermosome to the MgATP-bound state, appears to be con-

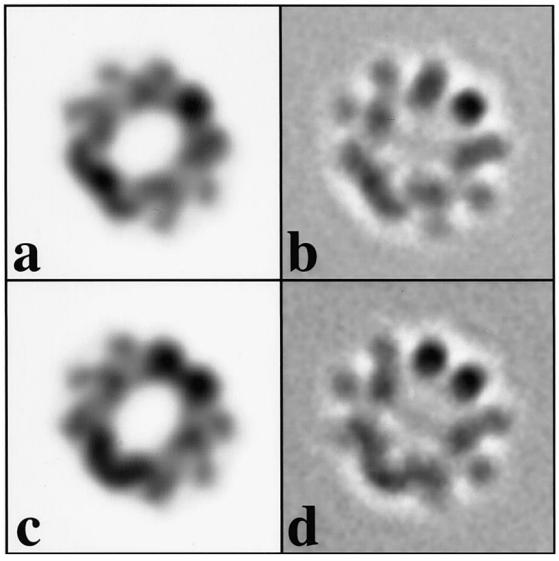

Fig. 2. Open state of the ATP- thermosome as revealed by model calculations. a,c: Calculated 20° tilted projections of the open cryo-EM structure of the α-only thermosome at two different azimuthal angles. b,d: Experimentally observed class-averages of (b) 1113 ATP-bound particles and (d) 749 ATP-bound particles each. Whatever the tilt angle, projections of either the asymmetric or the closed models are very different from the experimentally documented ones.

firmed by our cryo-EM data. Interestingly, cryo-EM analysis of GroEL in the absence of GroES shows that binding of ATP is accompanied by a twisting of the apical domains [6]. It is tempting to speculate that a twisting of the apical domains of the thermosome might move the hydrophobic patches on the protrusions outward. This, in turn, would result in a more pronounced tilting of the ATP-particles, attracted to the water–air interface at a slightly different angle.

In the crystal structure of the thermosome [5], like in the GroEL-GroES complex, the hydrophobic substrate-binding sites are buried in the intersubunit interface, whereas the cavity is lined with polar residues favorable to protein folding. Although it would also be consistent with the SANS data, we cannot currently determine whether the transient hydrolytic species we observe is indeed a closed one. Indeed, for this species, no markedly tilted classes could be visualized. This would either indicate that the top-view is a strongly preferred orientation, as in the case of the apo-chaperonin, or that we are unable to resolve the tilted classes due to their similarity to the non-tilted ones. The latter possibility would in itself be an indication of a closure.

In summary, even without performing a 3-D analysis, this study demonstrates a straightforward relationship between the nucleotide-bound state and the conformation of the *T. acidophilum* thermosome in vitrified ice (Fig. 3). Therefore, it provides a valuable supplement to the work of Schoen et al. [11], which yields 3-D reconstructions of the open, closed, and asymmetric forms of the nine-fold symmetric *S. shibatae* thermosome, but is unable to establish any correlation between a given form and a particular stage in the reaction cycle of this chaperonin. The reason for the difference between the cryo-EM behavior of the two thermosome species is unclear. All the particles of the apo-thermosome of *T. acidophilum* have the same, open conformation; all of them respond to nucleotide binding and hydrolysis by conformational rearrangements, which can be predictably regulated by the experimental setup. A potential advantage of our work resides in a parallel

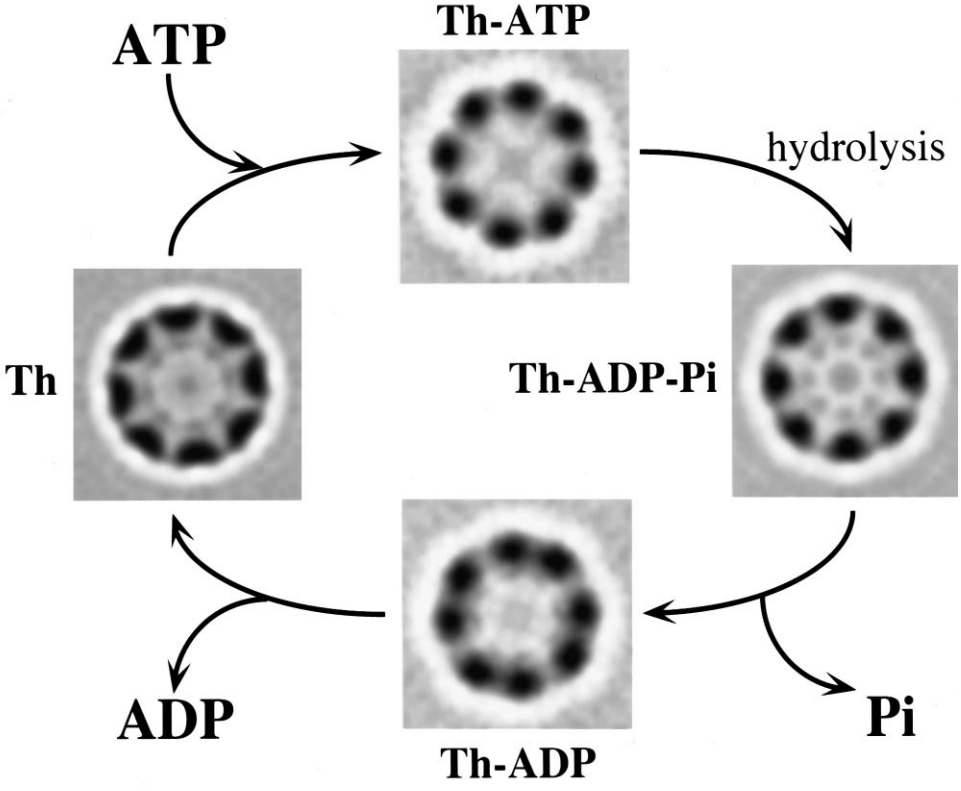

Fig. 3. Conformational rearrangements of the top-view projections of the thermosome upon ATPase cycling. Different nucleotide-bound states are represented by corresponding four-fold symmetrized top-view class-averages.

biochemical characterization of the *T. acidophilum* thermosome [17]; it ensures the nucleotide-free content of the apothermosome preparation and the effective nucleotide binding under the experimental conditions used, and identifies the nature of the nucleotide-bound species under examination.

Acknowledgements: Irina Gutsche thanks EMBO for a long-term postdoctoral fellowship.

References

[1] Hartl, F.U. (1996) Nature 381, 571–579.
[2] Sigler, P.B., Xu, Z., Rye, H.S., Burston, S.G., Fenton, W.A. and Horwich, A.L. (1998) Annu. Rev. Biochem. 67, 581–608.
[3] Gutsche, I., Essen, L.-O. and Baumeister, W. (1999) J. Mol. Biol. 293, 295–312.
[4] Klumpp, M., Baumeister, W. and Essen, L.O. (1997) Cell 91, 263–270.
[5] Ditzel, L., Lowe, J., Stock, D., Stetter, K.O., Huber, H., Huber, R. and Steinbacher, S. (1998) Cell 93, 125–138.
[6] Roseman, A.M., Chen, S., White, H., Braig, K. and Saibil, H.R. (1996) Cell 87, 241–251.
[7] Xu, Z., Horwich, A.L. and Sigler, P.B. (1997) Nature 388, 741–750.
[8] Llorca, O., Smyth, M.G., Carrascosa, J.L., Willison, K.R., Radermacher, M., Steinbacher, S. and Valpuesta, J.M. (1999) Nature Struct. Biol. 6, 639–642.
[9] Nitsch, M., Walz, J., Typke, D., Klumpp, M., Essen, L.O. and Baumeister, W. (1998) Nature Struct. Biol. 5, 855–857.
[10] Gutsche, I., Holzinger, J., Rößle, M., Heumann, H., Baumeister, W. and May, R.P. (2000) Curr. Biol. 10, 405–408.
[11] Schoen, G., Quaite-Randall, E., Jiménez, J.L., Joachimiak, A. and Saibil, H.R. (2000) J. Mol. Biol. 296, 813–819.
[12] Horwich, A.L. and Saibil, H.R. (1998) Nature Struct. Biol. 5, 333–336.
[13] Waldmann, T. et al. (1995) Eur. J. Biochem. 227, 848–856.
[14] Schagger, H. and von Jagow, G. (1987) Anal. Biochem. 166, 368–379.
[15] Dubochet, J., Adrian, M., Chang, J., Homo, J., Lepault, J., McDowall, A. and Schultz, P. (1988) Quart. Rev. Biophys. 21, 129–228.
[16] Hegerl, R. (1996) J. Struct. Biol. 116, 30–34.
[17] Gutsche, I., Mihalache, O. and Baumeister, W. (2000) J. Mol. Biol., in press.
[18] Nitsch, M., Klumpp, M., Lupas, A. and Baumeister, W. (1997) J. Mol. Biol. 267, 142–149.